

Comparison Of Algorithms For Agave Detection On Unmanned Aerial Vehicle Images

Jonathan Gabriel Escobar-Flores

Instituto Politécnico Nacional: Instituto Politecnico Nacional

Sarahi Sandoval (✉ sarahisandovale@gmail.com)

Instituto Politécnico Nacional: Instituto Politecnico Nacional <https://orcid.org/0000-0001-7221-5498>

Eduardo Gámiz-Romero

Instituto Politécnico Nacional Centro Interdisciplinario de Investigación para el Desarrollo Integral:
Instituto Politecnico Nacional Centro Interdisciplinario de Investigacion para el Desarrollo Integral

Research Article

Keywords: algorithms, agave crops, drone, image segmentation, supervised classification, OBIA

Posted Date: July 8th, 2021

DOI: <https://doi.org/10.21203/rs.3.rs-624586/v1>

License: © ⓘ This work is licensed under a Creative Commons Attribution 4.0 International License.

[Read Full License](#)

38 **Abstract**

39

40 In this study, six supervised classification algorithms were compared. The algorithms were based on cluster
41 analysis, distance, deep learning and object-based image analysis. Our objective was to determine which of
42 these algorithms has the highest overall accuracy in both detection and automated estimation of agave cover in
43 a given area to help growers manage their plantations. An orthomosaic with a spatial resolution of 2.5 cm was
44 derived from 300 images obtained with a DJI Inspire 1 unmanned aerial system. Two training classes were
45 defined: 1) sites where the presence of agaves was identified, 2) “absence”; where there were no agaves but
46 other plants were present. The object-oriented algorithm was found to have the highest overall accuracy (0.963),
47 followed by the support-vector machine with 0.928 accuracy and the neural network with 0.914. The algorithms
48 with statistical criteria for classification were the least accurate; Mahalanobis distance = 0.752 accuracy and
49 minimum distance = 0.421. We recommend that agave plantation managers use drones for their efficiency and
50 speed. We further recommend that the object-oriented algorithm be used, because in addition to having the
51 highest overall accuracy for the image segmentation process, it yields parameters that are useful for estimating
52 the coverage area, size, and shapes, which can aid in better selection of agave individuals for harvest.

53

54 Keywords: algorithms, agave crops, drone, image segmentation, supervised classification, OBIA

55

56

57

58 **Introduction**

59

60 The genus *Agave* includes 204 species, of which 163 are distributed in Mexico (García-Mendoza et al. 2019).
61 Twenty-five species of agave have been recorded as being used to produce mezcal. The most used species are
62 wild; e.g., *A. durangensis*, *A. salmiana*, while some are cultivated; e.g., *A. angustifolia* (Carrillo-Trueba, 2007).
63 In the past two decades, the demand and overexploitation of agave for mezcal production has caused wild
64 populations to decline rapidly. One of the main reasons for the decline is that the plants are harvested before
65 sexual reproduction (Rangel-Landa et al., 2015). In Mexico, the main strategy to restore wild and cultivated
66 agave populations is assisted recovery, which consists of in vitro germination and subsequent transfer to
67 restoration sites (Rangel-Landa et al., 2015). However, agave population parameters, including growth rate,
68 recruitment, and presence of nurse plants, are mainly monitored manually, which involves considerable effort
69 (Calvario et al., 2020).

70

71 Agaves can be detected and counted by applying algorithms to digital images captured from unmanned aerial
72 vehicles (UAVs). These techniques are widely used in precision agriculture (Tsouros et al., 2019). UAVs can
73 provide high resolution images (1–2 cm), depending on the height of the flight and the focal length of the camera
74 (Torres-Sánchez et al., 2015). This has been very useful for counting and morphometric analysis of agaves; for
75 example, Calvario et al. (2020) conducted a blue agave count using images taken from a DJI Phantom 4 UAV,
76 and applied an algorithm based on mathematical morphology. They found that the estimate of the number of
77 plants identified automatically in the images had an overall precision between 0.830 and 0.980. Another recent
78 study, also carried out with blue agave, was Flores et al. (2021). They applied a convolutional neural network
79 (CNN), in which patterns and textures are learned, and used to carry out automated counts in images taken from
80 UAVs. They report a level of precision of 0.96 for the agave count in their study.

81 As mentioned above, detection and counting has only been carried out for blue agaves using deep learning
82 algorithms, which require robust knowledge of image processing by users. This study therefore set out to
83 compare supervised classification algorithms for first-time detection of *cenizo* agaves (*Agave durangensis*),
84 which are in danger of extinction. We compared algorithms based on statistical rules that are commonly used
85 in remote sensing, and deep learning algorithms that are available and contain flowcharts in commercial and
86 free software.

87 **Materials and methods**

88 The Sampling was carried out in the Ejido Nombre de Dios, Durango, that is located at coordinates 23 ° 36 'and
89 24 ° 05' north latitude, and 103° 56 'and 104 ° 25 'west longitude, at an altitude of 1800 m (Figure 1). In
90 September 2020 along of 10 hectares of *Agave durangensis*, the aerial survey was carried out using a DJI Inspire
91 V.2 UAS (unmanned aerial system) equipped with camera ZenmUSE x3, with a 20 minutes of flight time. To
92 capture images, we use the DJI GS Pro (GSP) application performing the missions with the 3Dmap Area mode.
93 The flight parameters for 10 hectares of coverage using 2 sets of batteries were: definition of 8 lines of course
94 count, the image capture mode was hover and capture at point, flight course mode Inside. The side overlap ratio
95 was a 70% and gimbal angle 90 degrees. The speed of the aircraft was 4.0 m / s and flight height of 50 meters.
96
97
98

99
100
101
102
103
104
105
106
107
108
109
110
111
112
113
114
115
116
117
118
119
120
121
122
123
124
125
126
127
128
129
130
131
132
133
134
135
136
137
138
139
140
141
142
143
144
145
146
147
148
149

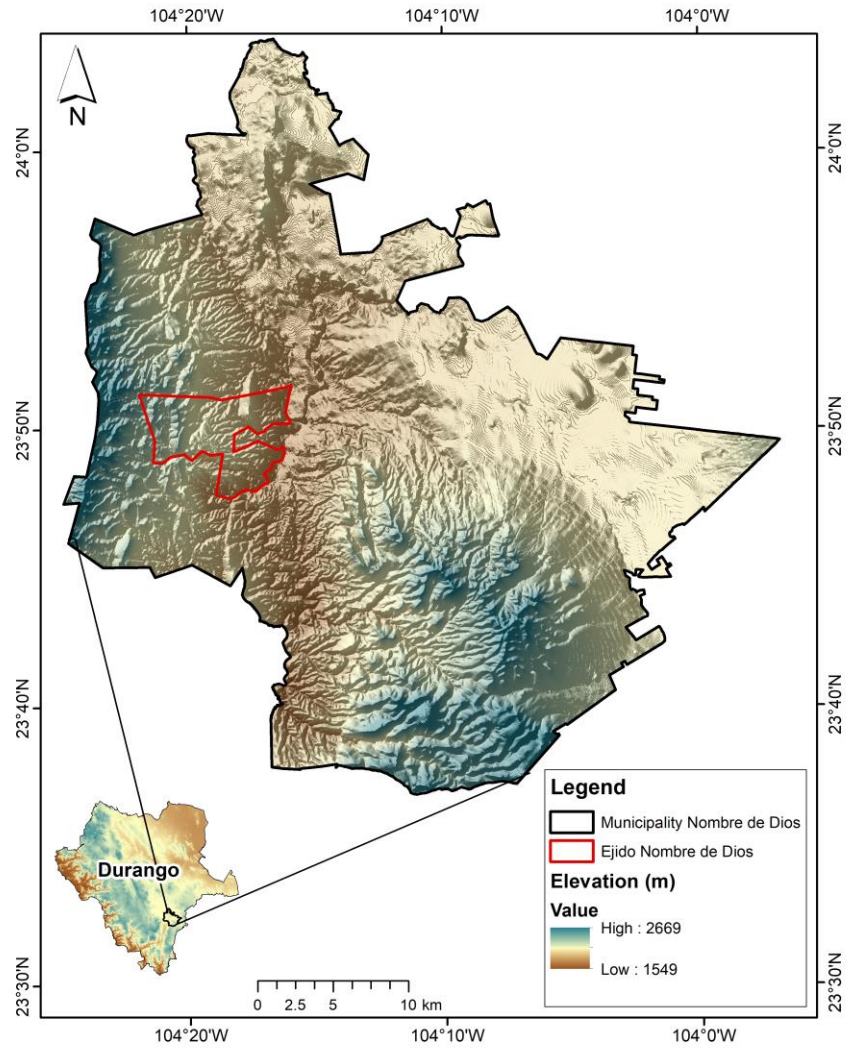


Figure 1. Map of study area of Municipality Nombre de Dios, Durango.

Image processing

The images were georeferenced with DATUM WGS84 Zone 13 using Agisoft Photoscan. To generate orthomosaic the photographs were oriented, establishing 50,000 key points per photograph, and 5,000 link points per photo, generating a point cloud with more than 1 million points. Orthomosaic with a spatial resolution of 2.5 cm/px were derived from the point cloud. The Orthomosaic was exported in JPG format for the supervised classifications in the program ENVI 5.3.

150 **Training sites**

151

152 A stratified random sampling method (Olofsson et al., 2014) was used to generate the reference data in ArcGis.

153 A total of 860 random points were sampled, with at least 430 points for each class (Goodchild, 1994). The

154 following classes were considered: class a is presences of agaves mescaleros with 430 sites, class b is absences

155 of agaves with sites. These data were contrasted with the category to which each training pixel belongs,

156 corresponding to Georeferenced sites (Datum WGS-84, 13N) obtained in the field in September 2020.

157 **Classification methods**

158 *Statistical rule-based algorithms.* We used three types. The first was minimum distance, which uses the mean

159 vectors of each region of interest (ROI) and calculates the euclidean distance from each unknown pixel to the

160 mean vector for each class. Pixels are put into the closest ROI class unless the user specifies standard deviation

161 or distance thresholds, in which case some pixels may be unclassified if they do not meet the specified criteria.

162 The second algorithm was Mahalanobis distance. This is a direction-sensitive distance classifier that uses

163 statistics for each class. It assumes all class co-variances are equal and therefore is a faster method. The third

164 algorithm uses maximum likelihood. This method assumes that the statistics for each class in each band are

165 normally distributed and calculates the probability that a given pixel belongs to a specific class. Unless a

166 probability threshold is selected, all pixels are classified. Each pixel is assigned to the class with the highest

167 probability. The ROIs correspond to the sites with presence or absence of mezcal agaves (Richards, 1999).

168 *Deep learning algorithms.* We used two types. The first was a back-propagation artificial neural network

169 (BPNN) (Tan and Smeins, 1996). BPNN is widely used because of its structural simplicity and robustness in

170 modeling non-linear relationships. The first step in BPNN supervised classification is to enter the input layer,

171 which in this study corresponds to the values of the pixel image from the UAV. Weights are then assigned to

172 the BPNN to produce analytical predictions from the input values. We used a logistic function and a training

173 rate of 0.20, previously applied in land cover classification (Hepner et al., 1990; Braspenning & Thuijisman,

174 1995). The output layer comprised two neurons representing the class of presences or absences of mezcal

175 agaves.

176 The second type was a support vector machine algorithm. This method is based on statistical learning theory,

177 and often yields good classification results from complex and noisy data. It separates the classes with a decision

178 surface that maximizes the margin between the classes. The surface can be called the optimal hyperplane, and
 179 the data points closest to the hyperplane are called support vectors. The support vectors are the critical elements
 180 of the training set. We used the ENVI implementation of SVM, which uses the *pairwise* classification strategy
 181 for multiclass classification (Hsu et al. 2010).

182 *Object-Based Image Algorithm (OBIA)*. The mezcal agaves were detected using OBIA, a digital analysis of
 183 images in which spatially and spectrally similar pixels are clustered into groups called objects in order to then
 184 carry out more precise classifications on multispectral images (Blaschke, 2010). The datasets used were the
 185 image mosaic with 2.2 cm spatial resolution. The first pass was segmentation of the images using *rule-based*
 186 *feature extraction* in ENVI 5.3, following the workflow: edge scale level 80%; merge settings full lambda
 187 schedule 90%. The segmentation was begun using the Full Lambda-Schedule algorithm created by Robinson
 188 et al. (2002). The algorithm iteratively merges adjacent segments base on a combination of spectral and spatial
 189 information (Eq. 1), where O_i is región i of the image, $[O_i]$ is the área of región i , U_i is the average value in
 190 región i . U_j is the average value in región j . $\|U_i - U_j\|$ is the Euclidean distance between the spectral values of
 191 regions i and j , and of $(\partial(O_i, O_j))$ is the length of the common boundary of O_i and O_j .

192

193

$$t = \frac{[O_i] \cdot [O_j] \cdot \|U_i - U_j\|^2}{length(\partial(O_i, O_j))} \quad Eq. 1$$

194 The segmentation yielded polygons with similarities in size and shape to agaves. The spatial attributes were
 195 analyzed based on a smoothed version of the geometry, not the original geometry (Douglas and Peucker, 1973).

196 **Validation**

197 The classifications were cross-validated (10-fold) estimated the uncertainty of the classification using estimated
 198 error matrix in terms of proportion of area and estimates of overall map accuracy (\hat{O}), user's accuracy (\hat{U}_i) (or
 199 commission error) and producer's accuracy (\hat{P}_j) (or omission error) recommended by Olofsson et al. (2014): p_{ij}
 200 is defined as a cell entry of error matrix of i map classes. A poststratified estimator of p_{ij} is (Eq. 2):

$$\hat{p}_{ij} = W_i \frac{n_{ij}}{n_i} \quad (2)$$

where W_i is the proportion of the area mapped as class i . n_i is the total number of sample units in map
 class i . n_{ij} is the sample count at cell (i,j) in the error matrix.

201 $\hat{p}_{.j}$ is a poststratified estimator for simple random and systematic sampling (Eq. 3):

$$\hat{p}_{.j} = \sum_{i=1}^q W_i \frac{n_{ij}}{n_{i.}} \quad (3)$$

202 where q is the class number.

203 An unbiased estimator of the total area of class j is then (Eq. 4):

$$\hat{A}_j = A \cdot \hat{p}_{.j} \quad (4)$$

204 where A is the total map area. For $\hat{p}_{.j}$, the standard error is estimated by (Eq. 5):

$$S(\hat{p}_{.j}) = \sqrt{\sum_{i=1}^q W_i^2 \frac{\frac{n_{ij}}{n_{i.}} \left(1 - \frac{n_{ij}}{n_{i.}}\right)}{n_{i.} - 1}} \quad (5)$$

205 The standard error of the error-adjusted estimated area is (Eq. 6):

$$S(\hat{A}_j) = A \cdot S(\hat{p}_{.j}) \quad (6)$$

206 Finally (Eq. 7),

$$\hat{A}_j \pm 1.96 \cdot S(\hat{A}_j) \quad (7)$$

207 presents an approximate 95% confidence interval.

208 The \hat{O} , \hat{U}_i and \hat{P}_j were calculated with Eqs. (8-10) (Congalton, 1991). \hat{U}_i of class i is the proportion of the area

209 mapped as class i that has reference class i . \hat{P}_j of class j is the proportion of the area of reference class j that is

210 mapped as class j .

$$\hat{O} = \sum_{j=1}^q \hat{p}_{jj} \quad (8)$$

$$\hat{U}_i = \frac{\hat{p}_{ii}}{\hat{p}_{i.}} \quad (9)$$

$$\hat{P}_j = \frac{\hat{p}_{jj}}{\hat{p}_{.j}} \quad (10)$$

211

212

213 **Results and Discussion**

214

215 The supervised classifications obtained using the algorithms with statistical rules had the lowest overall
216 precision; in fact, a very low precision of 0.421 was obtained with the minimum distance algorithm, in addition
217 to overestimation of the area covered by agave (Table 1, Figure 2). For the Mahalanobis distance and maximum
218 likelihood algorithms, which use similar classification criteria, Mahalanobis was slightly better with an overall
219 precision of 0.752. However, this precision is lower than that reported by Carbvalho-Júnior et al. (2011) and
220 Talukdar et al. (2020), who report an overall precision of 0.82 to 0.89 in studies of land use and land use
221 changes. One of the disadvantages of using the Mahalanobis distance algorithm is that it assumes that the
222 histograms of the RGB bands have a normal distribution (Perumal and Bhaskaran, 2010), and when this
223 condition is not met, the overall precisions tend to have lower values, such as the value we report in the present
224 study.

225 The statistical rule algorithms had the highest errors of omission and commission for agave detection (Table 1,
226 Figure 2). For example, the maximum likelihood algorithm assumes Gaussian multivariate distributions for the
227 classification of the data, but the data in the feature space might not follow the assumed model. Moreover, it is
228 possible that a single class may be represented in multiple places in the feature space (Atkinson and Tatnall,
229 1997). This particularly affects the analysis when classes are amalgamated at a higher level in the classification
230 system; for example, if shrubs, grasses, and agaves are grouped together (Benediktsson et al., 1993).

231 The BPNN and SVM deep learning algorithms improved the classification, yielding overall precision levels
232 greater than 0.90 (Table 1). There was less confusion of agaves with other elements of the habitat in the images;
233 however, these algorithms were not perfect since some false positives were found (Figure 2). We achieved
234 slightly lower precision in the detection of agaves with BPNN than that reported by Flores et al. (2021) with
235 the convolutional neural network algorithm (overall precision 0.95), which has the ability to learn patterns and
236 textures. Estimation of the agave area also improved with the deep learning algorithms; the estimation error
237 was less than 40 m² when compared with the estimate obtained in the field (Table 1). The algorithm with the
238 best overall precision and the lowest error in estimating agave area was OBIA, with an overall precision of 0.96,
239 which is slightly better than that reported by Calvario et al. (2020) and Flores et al. (2021) for the detection of
240 blue agave. The deep learning algorithms used in this study have the advantage that during the classification

241 process they start from a distribution-free assumption; that is, no underlying model is assumed for the
 242 multivariate distribution of class-specific data in the feature space.

243

Table 1. Error matrix of two classes with cell entries (p_{ij}) based on Table 2 and expressed in terms of proportion area. Class a = presences of agave mezcalero Class b = absences

Algorithm	Class	References		Accuracy			Estimated map area (m ²)
		a	b	User's	Producer's	Overall	
Minimum distance	a	0.080	0.539	0.129	0.675	0.421	640.06 ± 12.05
	b	0.038	0.341	0.898	0.387		4751.88 ± 8.03
Mahalanobis distance	a	0.083	0.242	0.256	0.933	0.752	271.31 ± 4.66
	b	0.006	0.668	0.991	0.734		2767.78 ± 2.37
Máximum likelihood	a	0.079	0.265	0.229	0.993	0.733	249.95 ± 4.29
	b	0.005	0.654	0.999	0.711		2881.05 ± 0.75
BPNN	a	0.146	0.078	0.652	0.952	0.914	407.94 ± 4.88
	b	0.007	0.767	0.990	0.907		2237 ± 2.34
SVM	a	0.145	0.063	0.696	0.948	0.928	396.49 ± 4.50
	b	0.007	0.783	0.990	0.925		2193 ± 2.38
OBIA	a	0.135	0.030	0.814	0.960	0.963	345.89 ± 2.52
	b	0.005	0.828	0.993	0.964		2112.11 ± 1.94

244

245 In the estimation of errors in the counts of presence and absence of agaves using the Mahalanobis distance and
 246 maximum likelihood algorithms, the weight (W_i) assigned to absences was greater than 0.60, which affected
 247 estimation of the coverage both of area with agaves and area without the plant (Table 2). The W_i were low in
 248 the agave-present class in the deep learning and OBIA algorithms (Table 2). This makes sense, because agaves
 249 cover less than 20% of the area studied and therefore the estimate of agave coverage improves notably (Figure
 250 2).

251

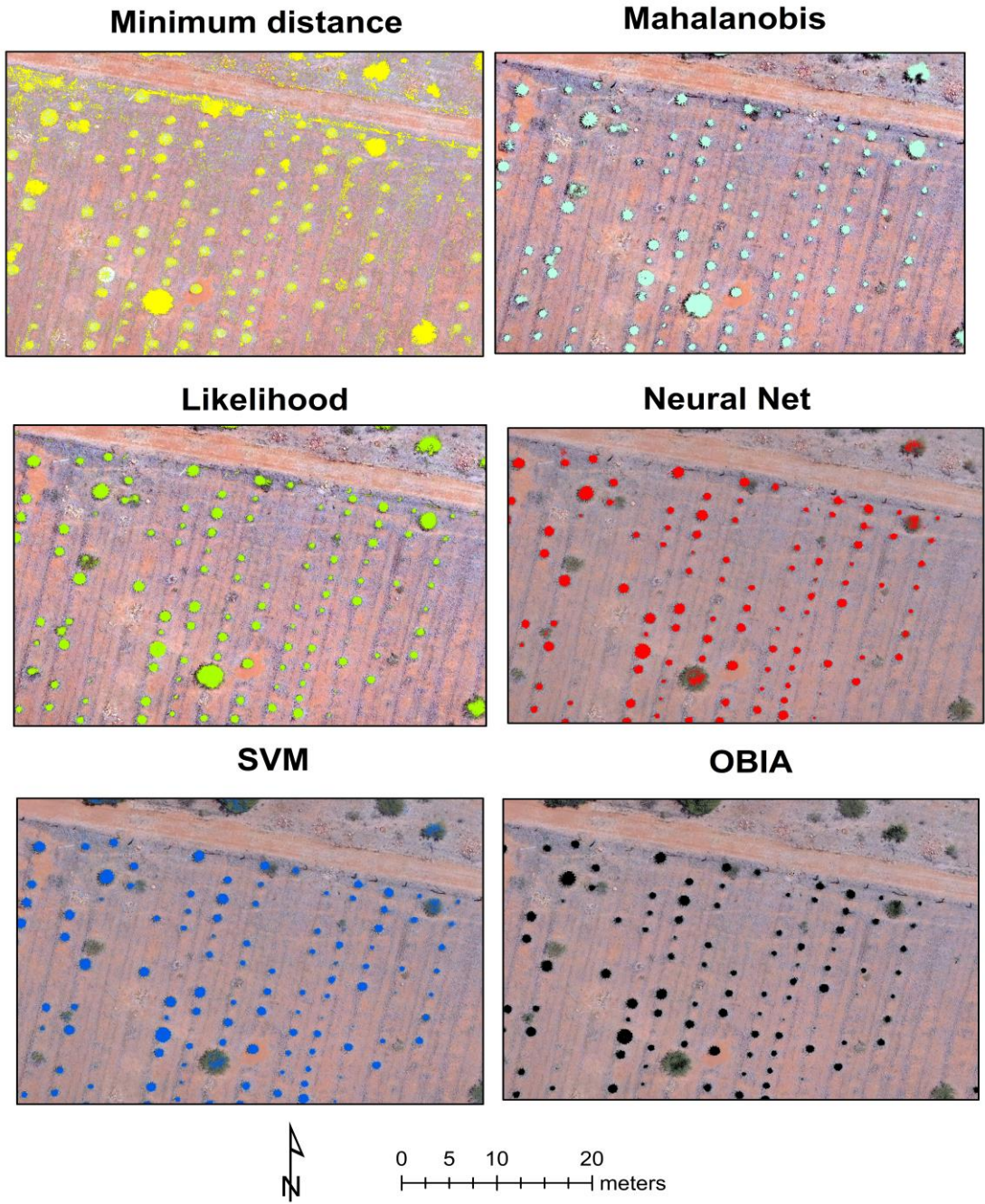
252

253

254

Table 2. Estimated error matrix based of sample counts (n_{ij}) from the accuracy assessment sample. Class a = presences of agave mezcalero Class b = absences

Algorithm	class	Total	Wi
Minimum distance	a	44619	0.619
	b	47079	0.380
Mahalanobis distance	a	10082	0.325
	b	52309	0.674
Máximum likelihood	a	45740	0.345
	b	45958	0.657
BPNN	a	15215	0.225
	b	57622	0.774
SVM	a	14208	0.208
	b	58629	0.791
OBIA	a	22641	0.166
	b	59402	0.834



264

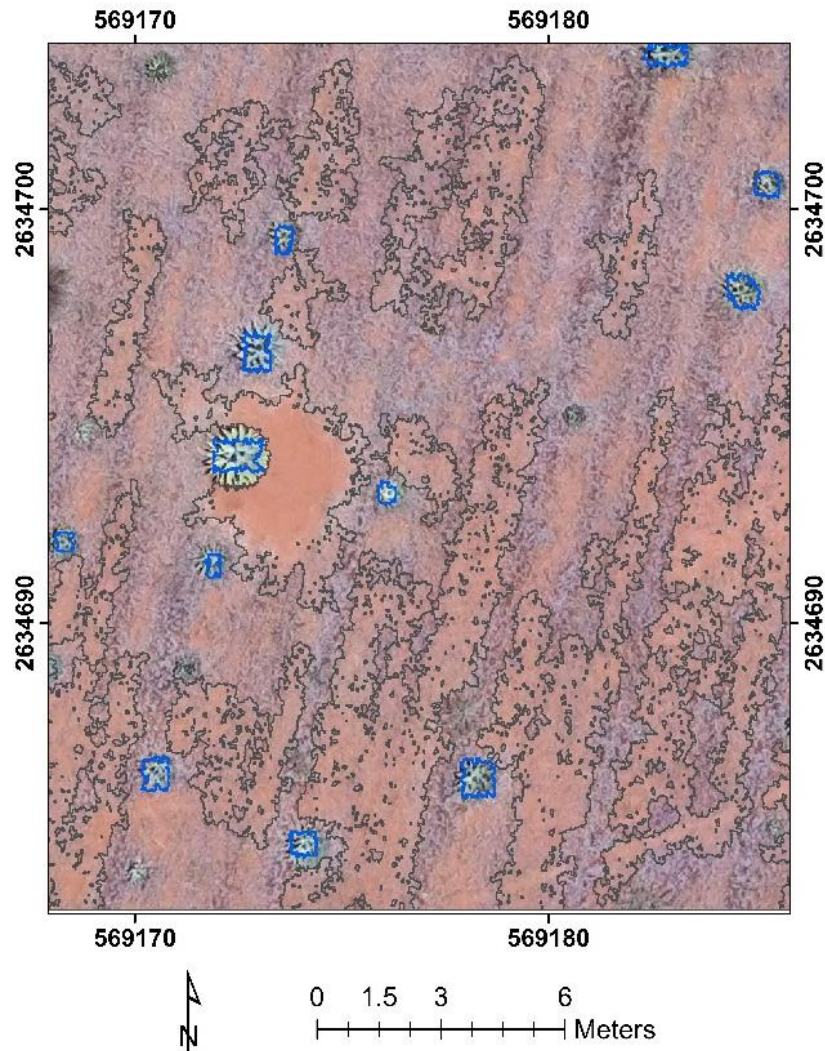
265

266 Figure 2. Supervised classifications obtained with the algorithms studied. Greater precision in the detection of
 267 agaves is observed with SVM and OBIA.

268

269 Segmentation of the image with OBIA clearly differentiated agave with cover greater than 30 cm from other
 270 elements of the habitat such as bare soil, grasslands and other herbaceous plants (Figure 3). A main advantage

271 of OBIA is that it has the ability to detect agaves of a variety of sizes and ages. The algorithm based on
272 mathematical morphology also has this ability (Jean-Philippe et al. 1994; Calvario et al., 2020).
273



274

275 Figure 3. Segmentation of the image of an agave (*Agave durangensis*) crop by the OBIA algorithm

276

277 Conclusion

278 The main difference between algorithms based on statistical rules and deep learning algorithms for the detection
279 of agaves is that the algorithms with a statistical approach depend on an assumed model, while the deep learning
280 algorithms depend on the training data and the histograms of the image. Therefore, we recommend using the
281 OBIA algorithm because it has three advantages over the other algorithms: 1) The global precision level is high

282 (> 0.90), which is useful in places where the possibility of confusing agaves with others plant species is high,
283 2) the result of the image segmentation process includes a database of shape parameters (roundness, elongation,
284 cover, compactness, etc.) with which a better selection of agaves can be made in the harvest 3) the Algorithm
285 OBIA is available in both commercial (ENVI) and free (SAGA) software giving you access to many
286 managements and researchers

287

288 **Acknowledgments**

289

290 I would like to meet Miss Gelvin Isela Gámiz Romero and Mr. Jose Cruz for allowing us to work on his
291 property

292

293

294 **Authors' contributions**

295

296 JE, and SS provide a substantial contribution to the conception and design of this mini-review. JE is the major
297 contributor of literature search and data analysis for this mini review. SS analyzed and interpreted the data for
298 this mini-review article. JE analyzed and interpreted the data for this mini-review article. SS is the major
299 contributor in drafting this mini review. EG contributed to critically revising the article for important intellectual
300 content. All the authors read and approved the final version of this mini-review and agree to approve for sending
301 for publication in this esteemed journal.

302

303 **Funding Open**

304

305 Access funding provided by Instituto Politecnico Nacional. CIIDIR Unidad Durango. Proyect Number

306

20210008

307

308 **Data availability** Not applicable.

309

310 **Compliance with ethical standards**

311

312 **Ethics approval and consent to participate** Not applicable.

313

314 **Consent for publication** Not applicable.

315

316 **Competing interests** The authors declare that they have no competing interests.

317

318

319

320

321

322

323 **References**

324

325 Atkinson PM Tatnall AR (1997) Introduction neural networks in remote sensing. *Int J Remote Sens.* 18(4):
326 699-709. <https://doi.org/10.1080/014311697218700>

327 Benediktsson JA Swain PH Ersoy OK (1993) Conjugate-gradient neural networks in classification of
328 multisource and very-high-dimensional remote sensing data. *Intl J Remote Sens.* 14(15), 2883-2903.
329 <https://doi.org/10.1080/01431169308904316>

330 Blaschke T (2010) Object based image analysis for remote sensing. *Photogram Rem S.* 65 (1): 2-16.
331 <https://doi.org/10.1016/j.isprsjprs.2009.06.004>

332 Braspenning PJ Thuijsman F (1995) *Artificial Neural Networks: An Introduction to ANN Theory and*
333 *Practice.* Springer Science & Business Media. New York.

334 Calvario G Alarcón TE Dalmau O Sierra B Hernandez C (2020) An Agave Counting Methodology Based on
335 Mathematical Morphology and Images Acquired through Unmanned Aerial Vehicles. *Sensors.* 20 (21):
336 6247. <https://doi.org/10.3390/s20216247>

337 Carrillo-Trueba LA (2007) Los destilados de agave en México y su denominación de origen. *Ciencias* 087.
338 <https://www.revistacienciasunam.com/es/>

339 Carvalho-Júnior OA Guimarães RF Gillespie AR Silva NC Gomes RA (2011) A new approach to change
340 vector analysis using distance and similarity measures. *Rem Sens.* 3(11): 2473-2493.
341 <https://doi.org/10.3390/rs3112473>

342 Congalton RG (1991) A review of assessing the accuracy of classifications of remotely sensed data. *Rem Sens*
343 *Environ.* 37(1):35–46. [https://doi.org/10.1016/0034-4257\(91\)90048-B](https://doi.org/10.1016/0034-4257(91)90048-B)

344 Douglas DH Peucker T (1973) Algorithms for the reduction of the number of points required to represent a
345 digitized line or its caricature. *Cartographica: the international journal for geographic information and*
346 *geovisualization.* 10 (2): 112-122. <https://doi.org/10.3138/FM57-6770-U75U-7727>

347 Flores D González-Hernández I Lozano R Vazquez-Nicolas JM Hernandez-Toral JL (2021) Automated Agave
348 Detection and Counting Using a Convolutional Neural Network and Unmanned Aerial
349 Systems. *Drones* 5(1): 4. <https://doi.org/10.3390/drones5010004>

350 García-Mendoza AJ Franco Martínez IS Sandoval-Gutiérrez D (2019) Cuatro especies nuevas de Agave
351 (Asparagaceae, Agavoideae) del sur de México. *Act Bot Mex*
352 126. <https://doi.org/10.21829/abm126.2019.1461>

353 Goodchild MF (1994) Integrating GIS and remote sensing for vegetation analysis and modeling:
354 methodological issues. *J. Veg. Sci.* 5(5):615–626. <https://doi.org/10.2307/3235878>

355 Hepner G Logan T Ritter N Bryant N (1990) Artificial neural network classification using a minimal training
356 set. Comparison to conventional supervised classification. *Photogram Eng Rem S.* 56 (4): 469–473

357 Hsu CW Chang CC Lin CJ (2010). A practical guide to support vector classification. National Taiwan
358 University. <http://www.csie.ntu.edu.tw/~cjlin/papers/guide/guide.pdf>.

359 Jean-Philippe T Marc-Olivier B Benoit MM Macq JM (1994) Automatic recognition of cancerous cells using
360 mathematical morphology. *Proc. SPIE* 2359, Visualization in Biomedical Computing 1994, (9
361 September 1994); <https://doi.org/10.1117/12.185200>

362 Olofsson P Foody GM Herold M Stehman SV Woodcock CE Wulder MA (2014) Good practices for estimating
363 area and assessing accuracy of land change. *Remote Sens Environ.* 148:42–57.
364 <https://doi.org/10.1016/j.rse.2014.02.015>

365 Perumal K Bhaskaran R 2010 Supervised classification performance of multispectral images. *Journal of*
366 *Computing.* 2(2): 124–129. <https://sites.google.com/site/journalofcomputing>. Accessed 28 July 2020

367 Rangel-Landa S Casas A Dávila P (2015) Facilitation of Agave potatorum: An ecological approach for assisted
368 population recovery. *For. Ecol. Manag.* 347: 57–74. <https://doi.org/10.1016/j.foreco.2015.03.003>

369 Richards JA (1999) *Remote Sensing Digital Image Analysis*. Springer-Verlag. Berlin

370

371 Robinson DJ Redding NJ Crisp DJ (2002) Implementation of a fast algorithm for segmenting SAR imagery.
372 Scientific and Technical Report. Defense Science and Technology Organization. Australia.
373 <https://apps.dtic.mil/sti/pdfs/ADA402611.pdf>. Accessed 12 February 2020

374 Talukdar S Singha P Mahato S Pal S Liou YA Rahman A 2020 Land-use land-cover classification by
375 machine learning classifiers for satellite observations—A review. *Rem Sens* 12 (7):1135.
376 <https://doi.org/10.3390/rs12071135>

377 Tan SS Smeins FE (1996) Predicting grassland community changes with an artificial neural network model.
378 *Ecol. Modell.* 84 (1–3):91–97. [https://doi.org/10.1016/0304-3800\(94\)00131-6](https://doi.org/10.1016/0304-3800(94)00131-6)

379 Torres-Sánchez J López-Granados F Serrano N Arquero O Peña JM 2015 High-throughput 3-D monitoring of
380 agricultural-tree plantations with unmanned aerial vehicle (UAV) technology. PloS one, 10(6):
381 e0130479. <https://doi.org/10.1007/s13593-016-0405-7>

382 Tsouros Dimosthenis C Stamatia Bibi Panagiotis G Sarigiannidis 2019 A review on UAV-based applications
383 for precision agriculture. Information. 10 (11): 349. <https://doi.org/10.3390/info10110349>

384
385
386

387
388
389
390
391
392
393